Available online at www.sciencedirect.com
ScienceDirect
Journal of Organometallic Chemistry 691 (2006) 4028–4041
Journal of Organometallic Chemistry
www.elsevier.com/locate/jorganchem

Synthesis, spectroscopy, structures and photophysics of metal alkynyl complexes and polymers containing functionalized carbazole spacers

Li Liu [a,b], Wai-Yeung Wong [b,*], Jian-Xin Shi [b], Kok-Wai Cheah [c], Tik-Ho Lee [b], Louis M. Leung [b]

[a] *Ministry of Education Key Laboratory for the Synthesis and Application of Organic Functional Molecules, Faculty of Chemistry and Chemical Engineering, Hubei University, Wuhan 430062, PR China*

[b] *Department of Chemistry and Centre for Advanced Luminescence Materials, Hong Kong Baptist University, Waterloo Road, Kowloon Tong, Hong Kong, PR China*

[c] *Department of Physics and Centre for Advanced Luminescence Materials, Hong Kong Baptist University, Waterloo Road, Kowloon Tong, Hong Kong, PR China*

Received 27 March 2006; received in revised form 5 June 2006; accepted 5 June 2006
Available online 15 June 2006

Abstract

A new class of soluble and thermally stable group 10 platinum(II) poly-yne polymers functionalized with 9-arylcarbazole moiety *trans*-[-Pt(PBu_3)$_2$C≡CRC≡C-]$_n$ (R = 9-arylcarbazole-3,6-diyl; aryl = *p*-methoxyphenyl, *p*-chlorophenyl) were prepared in good yields by the polycondensation polymerization of *trans*-[$PtCl_2(PBu_3)_2$] with HC≡CRC≡CH under ambient conditions. The optical absorption and emission properties of these polymetallaynes were investigated and compared with their bimetallic molecular model complexes *trans*-[Pt(Ph)(PEt_3)$_2$C≡CRC≡CPt(Ph)(PEt_3)$_2$] as well as their group 11 gold(I) and group 12 mercury(II) neighbors [(PPh_3)AuC≡CRC≡CAu(PPh_3)] and [MeHgC≡CRC≡CHgMe]. The structures of all the compounds were confirmed by spectroscopic methods and by X-ray crystallography for selected model complexes. The influence of the heavy metal atom and the 9-aryl substituent of carbazole on the evolution of lowest electronic singlet and triplet excited states is critically characterized. It was shown that the organic-localized phosphorescence emission can be triggered readily by the heavy-atom effect of group 10–12 transition metals (viz., Pt, Au, and Hg) with the emission efficiency generally in the order Pt > Au > Hg. These carbazole-based organometallic materials possess high-energy triplet states of 2.68 eV or higher which do not vary much with the substituent of 9-aryl group.

Keywords: Acetylide; Carbazole; Gold; Mercury; Platinum; Phosphorescence

1. Introduction

The use of carbazole chromophores offers exciting perspectives for the design of new molecular and polymeric materials for various optoelectronic applications [1]. Many carbazole derivatives have a sufficiently high triplet energy to be able to host red [2–5], green [6,7], and in some cases even blue [8,9] triplet emitters. Poly(carbazole) homopolymers and their copolymers are highly promising materials for applications in light-emitting devices because they contain a rigid biphenyl unit which can lead to a large band gap with efficient blue emission, and the facile substitution at the remote *N*-position offers the possibility of improving the solubility and processability of polymers without remarkably increasing the steric interactions in the polymer backbone [1].

While developments based on the exploitation of 9-arylcarbazole as the building unit for the synthesis of branched molecules, oligomers, polymers or even dendrimers have been extensive, most of them are restricted to purely organic systems [10]. Carbazole-based coordination/organometallic compounds have been much less explored [11]. To our knowledge, carbazole-containing

* Corresponding author. Tel.: +852 3411 7074; fax: +852 3411 7348.
E-mail address: rwywong@hkbu.edu.hk (W.-Y. Wong).

0022-328X/$ - see front matter © 2006 Elsevier B.V. All rights reserved.
doi:10.1016/j.jorganchem.2006.06.006

metal alkynyl compounds are still scarce. Literature examples are exclusively confined to 2,7-diethynyl-9-butylcarbazolediyl-spaced metal di-, oligo- and polymers [12]. However, there has been no report of 9-arylcarbazolyl-derived metal complexes, and the chemistry of such compounds would be interesting within the realm of materials science and optoelectronics. There are also very few reports in the sensitization of carbazole's triplet emission using heavy-metal effects [10h]. According to the energy gap law, the rate of phosphorescence emission is increased by interruption of the π-conjugation, i.e. a compound with high-energy triplet state is desirable [13]. With this in mind, we report here the synthesis, spectroscopic characterization, crystal structures and photophysical properties of some luminescent group 10–12 dinuclear and polynuclear platinum(II), gold(I) and mercury(II) complexes functionalized with some 9-arylcarbazole spacers. The influence of the heavy metal center and the 9-aryl substituent of carbazole ring on the photoluminescence behavior will be elucidated in this contribution.

2. Results and discussion

2.1. Synthesis

The synthesis of 3,6-diethynyl-9-arylcarbazole, **Ia** and **Ib**, are outlined in Scheme 1. First, the *N*-arylation of carbazole was achieved by the modified Ullmann condensation between carbazole and the corresponding *p*-iodoarene under the CuI/phen/KOH catalytic medium [14]. The corresponding *N*-arylated 3,6-dibromocarbazole precursors were obtained in good yields by bromination of 9-arylcarbazole derivatives with *N*-bromosuccinimide (NBS). An alternative synthetic method can also be used to produce 3,6-dibromo-9-arylcarbazoles in a similar yield by condensing the commercially available 3,6-dibromocarbazole with the corresponding *p*-iodoarene. The 3,6-bis(trimethylsilylethynyl)-functionalized 9-arylcarbazole compounds were formed from the Sonogashira-type coupling reaction between the dibromo derivatives and trimethylsilylacetylene and they were then converted to the diethynyl counterparts **Ia** and **Ib** in very good yields (88–94%) using K_2CO_3 in MeOH as the deprotecting reagent [15]. The crude products from these reaction mixtures were purified by passage through silica gel column and were recrystallized where necessary.

All the metal alkynyl complexes and polymers were obtained in good yields by the general alkynylation routes as described in Scheme 1. The diplatinum complexes can be considered the geometrical molecular models for the long chain organometallic polymers. Organic ligands **Ia** and **Ib** were employed as versatile synthons in the present study to form a series of group 10–12 metal acetylide complexes and polymers by adaptation of the classical dehydrohalogenation procedures reported in the literature [16]. **1a**, **1b**, **2a** and **2b** were synthesized by CuI-catalyzed dehydrohalogenating coupling of *trans*-$[PtCl_2(PBu_3)_2]$ or *trans*-$[PtCl(Ph)(PEt_3)_2]$ with **Ia** or **Ib** at room temperature (r.t.), respectively. The feed mole ratios of 2:1 and 1:1 for the platinum chloride precursors and the diethynyl ligand were adopted for the model complex and polymer syntheses, respectively. Purification of the polymers **1a** and **1b** were accomplished by silica column chromatography using CH_2Cl_2 as the eluent whereas the diplatinum complexes **2a** and **2b** were isolated by preparative TLC on silica. We have also prepared the d^{10} digold(I) diacetylide counterparts **3a** and **3b** by reaction of $Au(PPh_3)Cl$ with **Ia** or **Ib** in a 2:1 stoichiometry in the presence of a base [17]. Similarly, complexes **4a** and **4b**, the isoelectronic and isolobal analogues of **3a** and **3b**, were synthesized by treatment of **Ia** and **Ib** with two equivalents of MeHgCl under similar basic medium [18]. The yields of these transformations are generally high in each case. All the new complexes and polymers are air-stable solids which can be stored without demanding any special precautions. They display good solubility in chlorocarbons such as CH_2Cl_2 and $CHCl_3$, but are insoluble in hydrocarbons. Estimates of the molecular weights using gel permeation chromatography (GPC) in THF indicate that the degrees of polymerization calculated from M_w are 8–16 for **1a** and **1b** (Table 1). It should be noted that the GPC method used does not give absolute values of molecular weights but can only measure the hydrodynamic volume. Rod-like polymers in solution possess different hydrodynamic properties than flexible polystyrene standard. So, calibration of the GPC with polystyrene is likely to inflate the values of the molecular weights of the poly-ynes to some extent.

2.2. Spectroscopic properties

The IR, NMR (^1H, ^{13}C and ^{31}P) and fast-atom bombardment (FAB) mass spectral data of our compounds agree with their chemical structures. The solution IR spectra are each characterized by a single sharp $\nu(C{\equiv}C)$ absorption band at ca. 2092–2134 cm^{-1}. The IR spectrum of each compound shows no $\nu(\equiv CH)$ band in the range 3200–3300 cm^{-1}, in line with the fact that **Ia** and **Ib** are completely being capped by the metal groups via σ bonds. The single $^{31}P\{1H\}$ NMR signals flanked by platinum satellites for **1a**, **1b**, **2a** and **2b** are consistent with a *trans* geometry of the square-planar Pt unit. The room-temperature ^{31}P NMR spectrum of **3a** and **3b** display a sharp singlet at δ 43.91, indicative of a symmetrical arrangement of PAuC≡C groups in solution. ^1H NMR resonances arising from the protons of the organic and phosphine moieties were clearly observed. The formulas of the model complexes **1a**, **1b**, **3a**, **3b**, **4a** and **4b** were also characterized by the presence of intense molecular ion peaks in their respective positive FAB mass spectra.

2.3. Crystal structure analyses

The three-dimensional molecular structures of **2a**, **3a** and **4b** were analyzed by X-ray crystallography and are

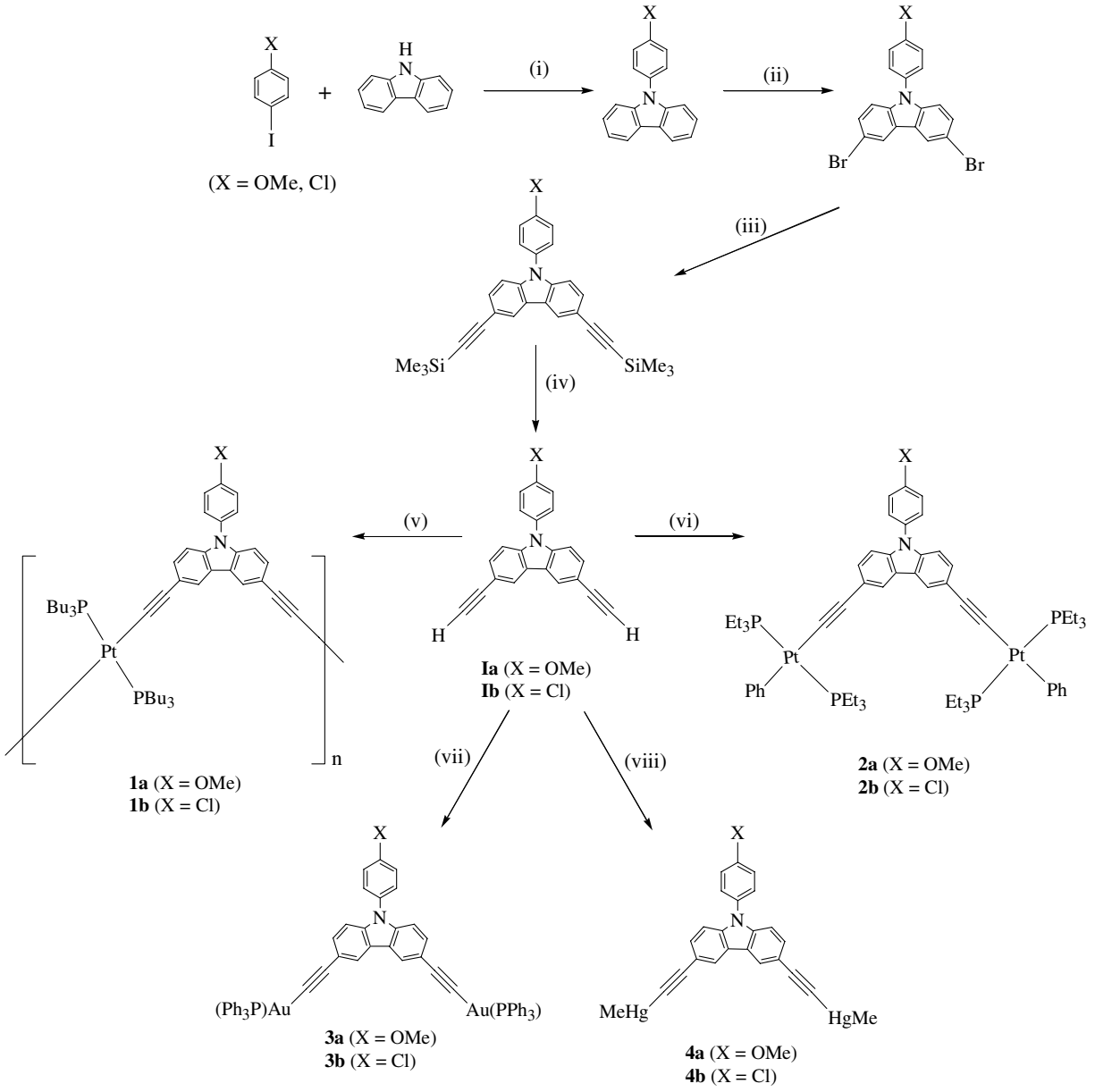

Scheme 1. (i) 1,10-phenanthroline, CuI, KOH, *p*-xylene, reflux; (ii) NBS, DMF, room temperature; (iii) trimethylsilylacetylene, $Pd(OAc)_2$, PPh_3, CuI, $^iPr_2NH$, reflux; (iv) K_2CO_3, MeOH, room temperature; (v) *trans*-$[PtCl_2(PBu_3)_2]$ (1 equiv), CuI, $^iPr_2NH$, room temperature; (vi) *trans*-$[PtPh(Cl)(PEt_3)_2]$ (2 equiv), CuI, $^iPr_2NH$, room temperature; (vii) $Au(PPh_3)Cl$ (2 equiv), NaOH/MeOH, room temperature; (viii) MeHgCl (2 equiv), NaOH/MeOH, room temperature.

Table 1
Structural and thermal properties of the polymers **1a** and **1b**

Complex	M_n[a]	M_w[b]	M_w/M_n	DP[c]	T_{decomp} (°C)[d]	% loss
1a	13,060	13,950	1.1	16	343 ± 5	25 (4Bu)[e]
1b	5550	6660	1.2	8	350 ± 5	38 (6Bu)[e]

[a] M_n = Number – average molecular weight.
[b] M_w = Weight – average molecular weight.
[c] DP = Degree of polymerization.
[d] Onset decomposition temperature.
[e] The groups eliminated are shown in parentheses.

depicted in Figs. 1–3 respectively. Pertinent bond distances and angles are given in Tables 2–4. In each case, the crystal structure consists of discrete binuclear molecules in which two terminal organometallic groups are linked by the 9-arylcarbazole-spaced bis(acetylide) moiety at the 3,6-position to afford the angular molecular skeleton. For the Pt(II) di-yne, there are two independent molecules per asymmetric unit in the unit cell and two half molecules of **4b** prevail in the unit cell of the Hg(II) complex. The coordination geometry at the platinum center in **2a** is square-planar with the two PEt_3 groups *trans* to each other and linear about the gold and mercury centers in **3a** and **4b**. The C≡C bond lengths in the ethynyl bridge [1.186(9)–1.27(2) Å] are fairly typical of metal-alkynyl σ-bonding [19]. The bond angles for the metal-alkynyl units are close to linearity.

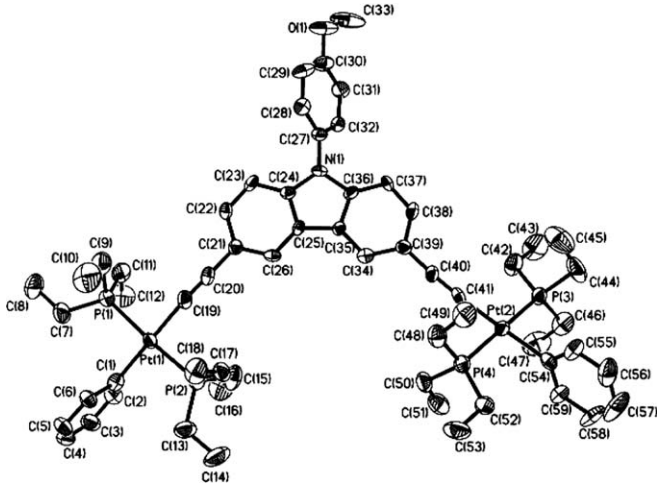

Fig. 1. Molecular structure of **2a**, with the atoms drawn at the 25% probability level.

The mean Pt–P and Pt–C(alkynyl) distances of 2.284(3) and 2.004(10) Å in **2a** are analogous to those previously reported for related platinum(II) alkynyls [19]. No apparent short intermolecular contacts or π-stacking interactions are observed in this Pt complex. The average Au–P bond length of 2.284(2) Å in **3a** is similar to those observed in other alkynylgold(I) phosphine complexes, but longer than those of the chlorogold(I) phosphines, in line with the higher *trans* influence of the alkynyl group [17]. The Au–C bond distances lie in the narrow range of 1.992(6)–2.010(7) Å. Apparently, aurophilicity is absent in **3a**, as the sterically bulky phenyl groups of the phosphine ligands probably prevent their close approach. While $[MeHg]^+$ is isoelectronic and isolobal with the $[(PPh_3)Au]^+$ fragment, both **3a** and **4b** have similar structural motifs. The Hg–C(alkyne) bond (2.017(19)–2.065(19) Å) is slightly longer than the Au–C(alkyne) bond (1.992(6)–2.010(7) Å).

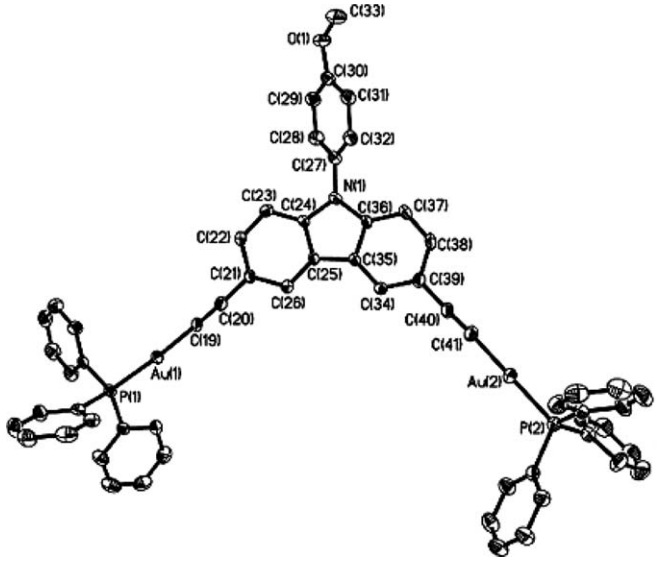

Fig. 2. Molecular structure of **3a**, with the atoms drawn at the 25% probability level.

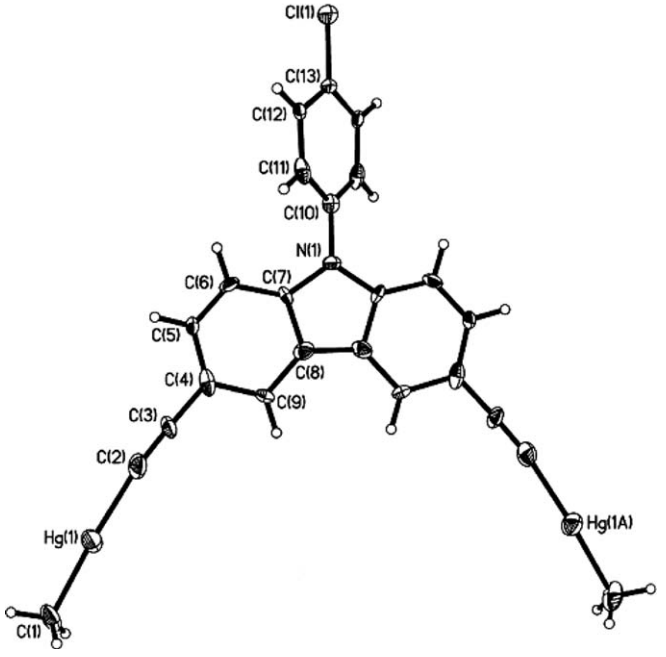

Fig. 3. Molecular structure of **4b**, with the atoms drawn at the 25% probability level.

Table 2
Selected bond lengths (Å) and angles (°) for **2a**

	Molecule 1	Molecule 2		Molecule 1	Molecule 2
Pt(1)–P(1)	2.281(3)	2.285(3)	Pt(1)–P(2)	2.285(3)	2.283(3)
Pt(1)–C(1)	2.012(10)	2.092(10)	Pt(1)–C(19)	1.989(11)	2.051(10)
Pt(2)–P(3)	2.280(3)	2.288(3)	Pt(2)–P(4)	2.282(3)	2.278(3)
Pt(2)–C(41)	1.960(9)	2.017(10)	Pt(2)–C(54)	2.039(9)	2.077(10)
C(19)–C(20)	1.205(14)	1.177(12)	C(20)–C(21)	1.455(13)	1.418(12)
C(40)–C(41)	1.257(12)	1.219(12)	C(39)–C(40)	1.409(12)	1.453(12)
N(1)–C(27)	1.401(11)	1.421(11)	C(30)–O(1)	1.376(12)	1.396(12)
P(1)–Pt(1)–P(2)	176.00(11)	174.05(12)	P(1)–Pt(1)–C(19)	88.2(3)	87.3(3)
P(2)–Pt(1)–C(19)	87.8(3)	88.8(3)	P(3)–Pt(2)–P(4)	177.13(11)	170.94(13)
P(3)–Pt(2)–C(41)	92.9(2)	92.2(3)	P(4)–Pt(2)–C(41)	86.7(2)	88.6(3)
Pt(1)–C(19)–C(20)	175.2(9)	174.9(8)	C(19)–C(20)–C(21)	177.5(9)	176.1(10)
Pt(2)–C(41)–C(40)	169.5(8)	169.1(8)	C(39)–C(40)–C(41)	176.7(10)	178.9(12)

Table 3
Selected bond lengths (Å) and angles (°) for **3a**

P(1)–Au(1)	2.2832(16)	P(2)–Au(2)	2.2845(19)
Au(1)–C(19)	1.992(6)	Au(2)–C(41)	2.010(7)
C(19)–C(20)	1.201(8)	C(20)–C(21)	1.443(8)
C(40)–C(41)	1.186(9)	C(39)–C(40)	1.459(9)
N(1)–C(27)	1.434(7)	C(30)–O(1)	1.360(8)
P(1)–Au(1)–C(19)	176.45(18)	P(2)–Au(2)–C(41)	175.3(2)
Au(1)–C(19)–C(20)	174.3(6)	Au(2)–C(41)–C(40)	175.4(6)
C(19)–C(20)–C(21)	176.6(7)	C(39)–C(40)–C(41)	177.6(7)

The Hg–CH_3 bond (2.058–2.059 Å) is slightly shorter than those observed in some methylmercury(II) complexes with thiol ligand (2.082–2.133 Å) [20]. The lattice structure of **4b** is highlighted by the ligand-unsupported mercurophilicity, and such interactions link the molecular units together to form an organized 3D polymeric network (Fig. 4). Remarkably, the whole lattice structure is fully supported and stabilized by extensive non-covalent d^{10}–d^{10} Hg···Hg interactive vectors (ca. 3.866 and 4.441 Å). Although the Hg···Hg contacts indicate that each of the individual interactions is relatively weak in nature, it is the large number of them that play a supramolecular role and generate a significant driving force for the observation of solid-state aggregation. There are good evidences that such mercurophilic forces are more than just van der Waals interactions in the present system. The van der Waals radius of mercury of up to 2.2 Å has been proposed [21]. So, the observed Hg···Hg separations are within the range of 3.71–4.25 Å for mononuclear [Hg(C≡CR)$_2$] (R = Ph, $SiMe_3$) [22], 3.738–4.183 Å for binuclear [MeHgC≡CRC≡CHgMe] (R = 9,9-dioctylfluorene-2,7-diyl and oligothienyl) [23] and 4.077 and 4.449 Å computed for molecular $(HgH_2)_n$ clusters ($n = 2,3$) [24] and are toward the upper limit of those accepted as representing metallophilic interactions [21]. As shown in Fig. 4, the lattice is characterized by infinite zig-zag chains of Hg atoms between adjacent molecules (e.g. Hg(2A)···Hg(1F)···Hg(1C)···Hg(1H) and Hg(1B)···Hg(1E)···Hg(1D)···Hg(1G)). This structure is unique in that no apparent weak Hg···η^2–C≡C interactions are observed which are commonly the driving force for the solid-state aggregation process to be observed in alkynyl complexes of CuI), Ag(I) and Hg(II) [18b,22b].

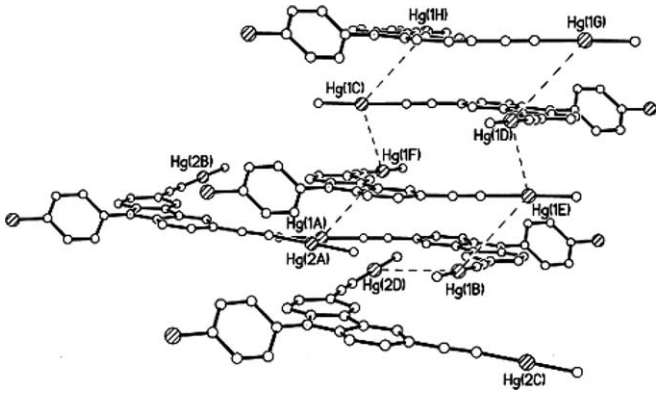

Fig. 4. Crystal packing diagram of **4b** in a 3D network, showing weak Hg···Hg interactions.

2.4. Thermal analysis

The thermal properties of the new metallopolymers were examined by thermogravimetric analysis (TGA) under nitrogen and both show good thermal stability with decomposition temperatures at 343–350 °C (Table 1). They are more thermally stable than that for the corresponding 9-butylcarbazole analogue (315 °C) [25], reflecting the advantage of attaching the aromatic rings to the carbazole nitrogen unit in enhancing the thermostability of these polymetallaynes. The degradation patterns for these polymers are very similar and the decomposition can be assigned to the loss of various number of butyl groups from the Pt poly-yne chains on the basis of the experimentally observed % weight loss. These metallopolymers did not display discernible glass transition in the DSC curves.

2.5. Electronic absorption and luminescence spectra

We found that the platinum-containing polymers can cast tough, free-standing thin films of good quality from appropriate solvents for optical characterization. The photophysical data of the new compounds measured in both solution and solid phases are tabulated in Table 5. All the metal alkynyls display similar structured absorption bands in the near UV region. The lowest energy bands are caused by the intraligand $^1(\pi\pi^*)$ transitions, possibly mixed with contribution from some admixture of metal orbitals [16a]. The 0–0 absorption peak is assigned as the transition from the S_0 to S_1 states, which are predominantly delocalized π and π^* orbitals. As compared to the band in CH_2Cl_2 for the ligand, we find that the position of the lowest energy absorption band is red-shifted after the inclusion of metal fragment in metal di-ynes and polymers. This reveals that π-conjugation is preserved through the metal site by mixing

Table 4
Selected bond lengths (Å) and angles (°) for **4b**

	Molecule 1	Molecule 2		Molecule 1	Molecule 2
Hg(1)–C(1)	2.059(16)	2.027(17)	Hg(1)–C(2)	2.065(19)	2.017(19)
C(2)–C(3)	1.19(2)	1.27(2)	C(3)–C(4)	1.40(2)	1.400(19)
N(1)–C(10)	1.42(2)	1.37(2)	Cl(1)–C(13)	1.716(18)	1.70(2)
Hg(1)–C(2)–C(3)	172.6(15)	171.1(15)	C(1)–Hg(1)–C(2)	176.1(7)	179.0(7)
C(2)–C(3)–C(4)	177.8(17)	176.1(14)			

of the frontier orbitals of metal and the ligand. The transition energies of the polymers **1a** and **1b** are lowered with respect to those of **2a** and **2b**, suggesting a well extended singlet excited state in the former. The optical absorption wavelengths of our compounds generally vary in the order **Ia**(**b**) < **4a**(**b**) < **3a**(**b**) < **2a**(**b**) < **1a**(**b**). In other words, the order of π-delocalization through the metal chromophore is Pt(II) > Au(I) > Hg(II). On the other hand, the absorption spectra were found to be independent of the nature of the aryl substituent on the carbazole ring, which are related to the notion that the carbazolyl unit is not effective in π-conjugation along the main chain. It is seen that carbazole tends to reduce conjugation relative to the $(C_6H_4)_2$-linked congeners, causing a blue-shift in the absorption maxima [26].

The thin film photoluminescence (PL) spectra of the new compounds were measured at various temperatures. In dilute fluid solutions at 290 K, we observe an intense purple-blue $^1(\pi\pi^*)$ emission peak near 400 nm for each of them which is assignable to fluorescence ($S_1 \rightarrow S_0$) due to the short emission lifetimes (in the nanosecond range) and the small Stokes shift between absorption and PL peaks. The excitation spectra correspond well to the corresponding absorption spectra. As the temperature is cooled down to 11 K, very intense organic-localized phosphorescence bands become dominant in the spectra. The large Stokes shifts of these lower-lying emission peaks from the dipole-allowed absorptions (Figs. 5 and 6), plus the long PL lifetimes all point to their triplet parentage, and they are assigned to the $^3(\pi\pi^*)$ excited states of the diethynylcarbazole core

Table 5
Electronic absorption and emission data for metal alkynyl complexes and ligands

Compound	λ_{max} (nm)[a]		E_g (eV)[b]	λ_{em} (nm)[c]		
	CH_2Cl_2	film		CH_2Cl_2[d] (290 K)	Film (11 K)	Frozen CH_2Cl_2 (77 K)[e]
1a	248 298 345	258 300 355	3.23	369* 399 (0.013, 6.6) 418	403*, 422* 462, 488, 511 545	454 (56.4) 478* 501*
1b	249 300 344	259 300 354	3.21	370* 402 (0.008, 2.0) 419*	402*, 419* 461, 509* 541*	452 (40.1) 475*, 502*
2a	259 (8.4) 301 (6.1) 329 (7.1)	260 302 334	3.46	384* 401 (0.028, 2.0) 418*	404*, 424* 456, 489* 502*	443 (47.2) 465*, 487*
2b	258 (8.9) 303 (6.3) 330 (9.0)	258 302 334	3.46	377 396 (0.029, 2.5) 415*	404*, 422* 454, 474*, 486*, 500	441 (85.3) 464*, 484*
3a	263 (6.1) 277 (4.6) 315 (7.5) 331* (4.8)	245 323 341	3.31	389 408 (0.019, 3.6)	390*, 412*, 455, 480, 496 535*	433 (25.4) 458*, 471*
3b	263 (6.3) 276 (5.0) 316 (8.8) 330* (6.1)	243 323 340	3.35	386 419 (0.020, 5.1)	390*, 410* 455, 485, 498	435 (47.7) 461*, 473*
4a	260 (5.4) 269 (4.5) 300 (6.8) 322* (2.5)	265 311 331	3.44	380 399 (0.007, 3.1) 420	384*, 404* 450, 477, 508*	427 (4.0) 453*
4b	260 (4.1) 298 (4.8) 320* (2.8)	266 310 330	3.45	373 389 (0.016, 6.5) 406	381*, 402* 423*, 451 481, 495* 521*	425 (47.6) 450*
Ia	255 (6.5) 288 (6.0)	258 293	3.84	369 385 (0.101) 402		
Ib	253 (3.0) 287 (2.9)	258 293	3.84	368 385 (0.107) 402		

[a] Extinction coefficients (10^4 M^{-1} cm^{-1}) are shown in parentheses.
[b] Estimated from the onset wavelength of the solid-state optical absorption.
[c] Asterisks indicate that emission peaks appear as shoulders or weak bands.
[d] Fluorescence quantum yields and lifetimes (in ns) shown in parentheses (Φ_F, τ_F) are measured in CH_2Cl_2 relative to anthracene.
[e] Phosphorescence lifetimes τ_P (in μs) at 77 K for the peak maxima are shown in parentheses.

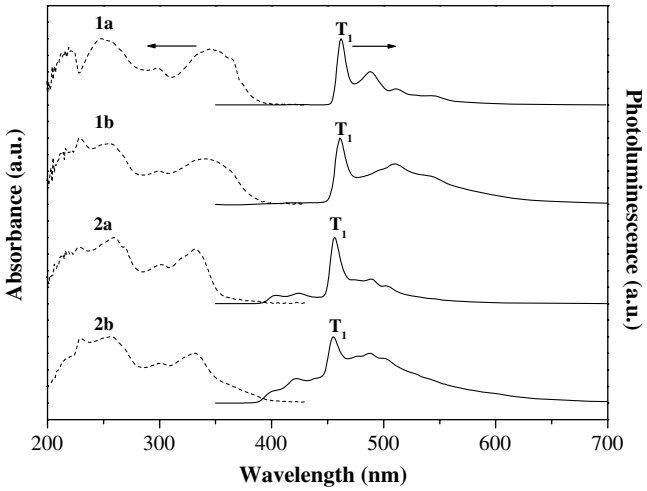

Fig. 5. Room temperature optical absorption spectra (in CH_2Cl_2) and the PL spectra of **1a**, **1b**, **2a** and **2b** (11 K in solid).

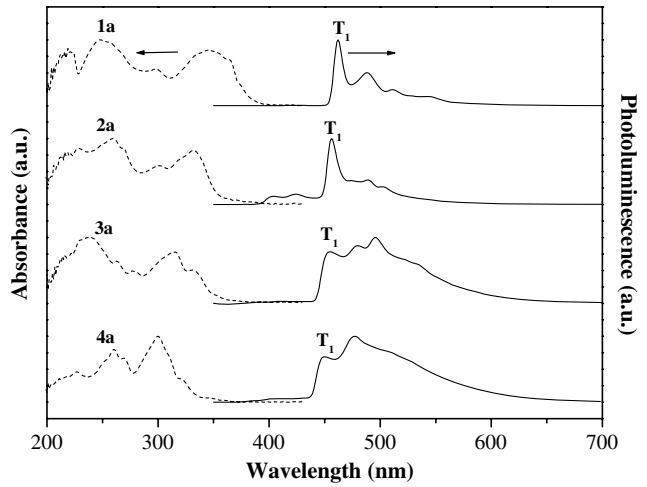

Fig. 6. Room temperature optical absorption spectra (in CH_2Cl_2) and the PL spectra of **1a**, **2a**, **3a** and **4a** (11 K in solid).

[16]. The assignment was also supported by the observed temperature dependence of the PL data, in accordance with earlier work on related metal alkynyls [16]. The temperature dependencies of the PL spectra for the polymers and some model complexes are displayed in Figs. 7–9. In each case, when the temperature is lowered, the triplet emission band increases in intensity sharply in contrast to the singlet emission and a well-resolved vibronic substructure becomes apparent. For instance, from 290 to 11 K, the singlet emission peak intensity increases only by a factor of 2.0 for **1a**, but the intensity of the lower-lying emission increases by a factor of 62.0. Such an intensity rise is indicative of a long-lived triplet excited state that is more sensitive to thermally activated non-radiative decay mechanisms. There is also a slight variation in the relative intensities of the vibronic structures with temperature for these compounds [16a]. The phosphorescence lifetimes (τ_P) at the peak maxima were found to be in the microsecond regime at 77 K (Table 5), in line with those for the phosphorescence

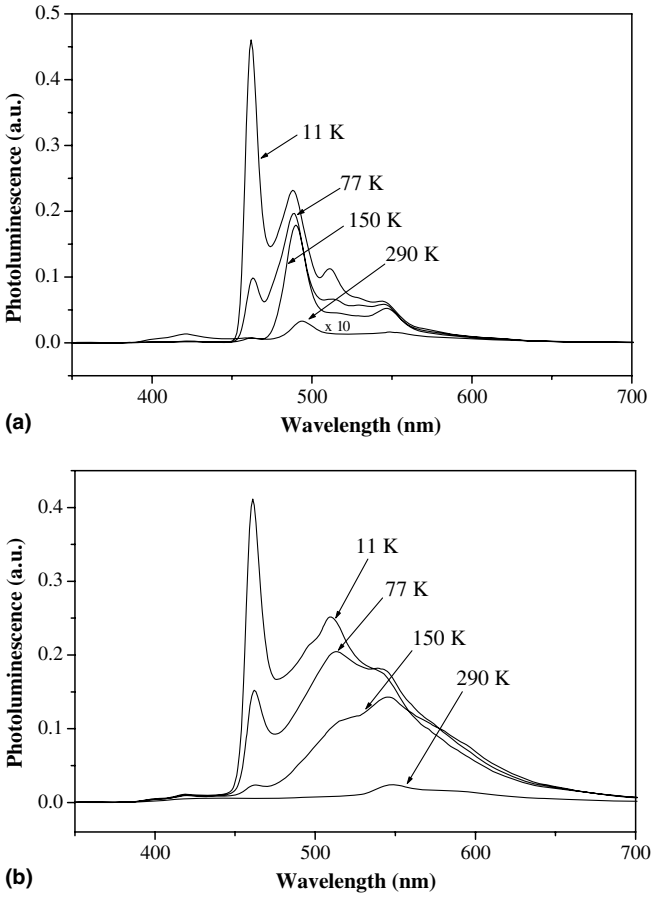

Fig. 7. Temperature dependence of the PL of (a) **1a** and (b) **1b**.

observed in similar systems reported in the literature [16a]. Compared with the solution PL data, the solid-state emission appears broad, structureless and red-shifted at room temperature for the mercury acetylide compounds, which is probably a result of interchain interactions due to aggregate formation [27]. This is also consistent with the X-ray structural data of **4b** (vide supra).

To examine the spatial extent of the singlet and triplet excitons in the present system, the energy gaps between S_0 and T_1 states were found to be 2.68–2.76 eV for our metal di-ynes and poly-ynes (Table 6). For these 9-arylcarbazole-spaced metallaynes, they exhibit high T_1 states $\geqslant$2.68 eV, which appear even higher than those bridged by some insulating Group 14 and 16 elements [13,28]. From Fig. 5, the phosphorescence spectra of the Pt compounds generally follow the same trends as the absorption features, in which the triplet emission peaks for the poly-ynes are slightly red-shifted relative to those for the di-ynes. It is obvious that the emission wavelength does not seem to vary much with the type of spacer group in each series. In addition, the energy of the $T_1 \rightarrow S_0$ transition changes with the type of the metal groups and the PL spectra of different metal complexes having the same organic chromophore are compared in Fig. 10. For each metal class, a strong phosphorescence band was observed due to the presence of strong spin–orbit coupling induced by the heavy metals,

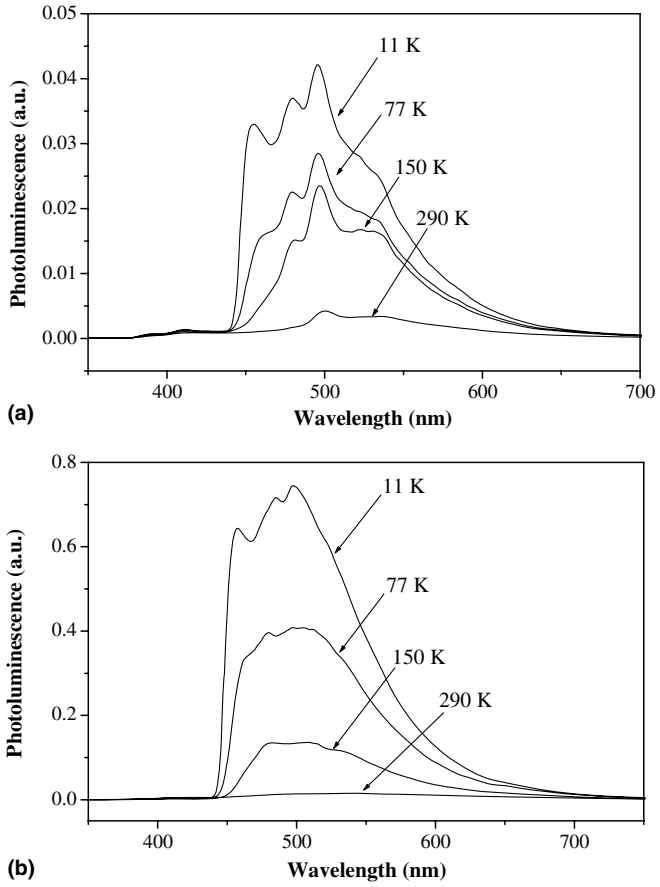

Fig. 8. Temperature dependence of the PL of (a) **3a** and (b) **3b**.

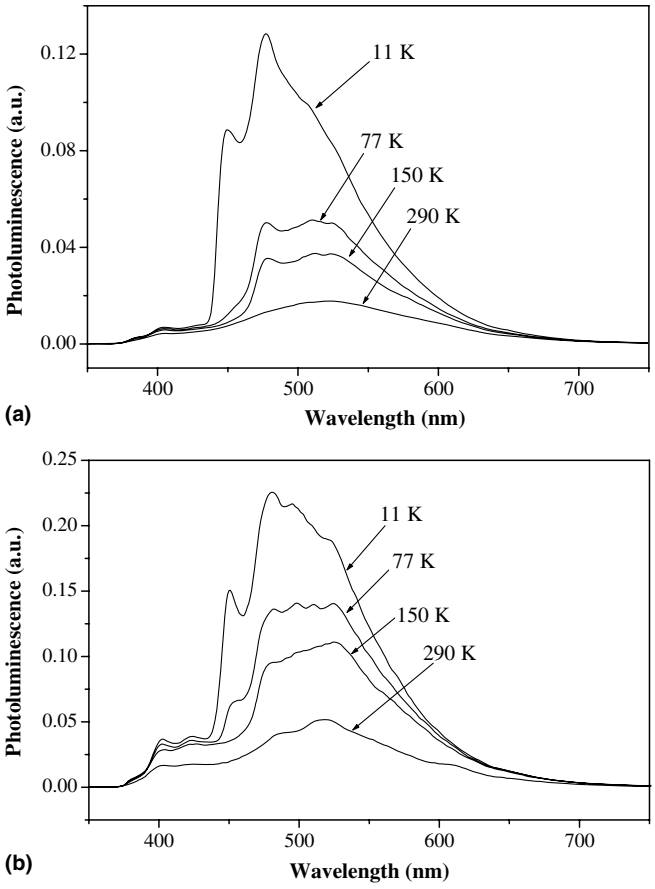

Fig. 9. Temperature dependence of the PL of (a) **4a** and (b) **4b**.

and there is a small but notable shift in the wavelength to the blue from Pt to Au followed by Hg, in line with the absorption trend. To access the relative intersystem crossing efficiency, the peak height ratio from triplet emission to singlet emission at 11 K, $\Delta E(S_1 \rightarrow S_0,\ T_1 \rightarrow S_0)$, was taken as a useful indicator (Table 6) [29]. We note a very high efficiency of triplet emission for the Pt polymers in each system and the intersystem crossing is much stronger in polymer than in the corresponding Pt di-yne. The order of S_1–T_1 crossover efficiency is roughly: **1a**(**b**) > **2a**(**b**) > **3a** (**b**) > **4a**(**b**). In other words, with the same ligand chromophore, the relative intersystem crossing rate or phosphorescence efficiency is the highest for the Pt(II) compounds and the lowest for the corresponding Hg(II) congener.

3. Concluding remarks

Our present work reports the synthesis and characterization of some group 10–12 metal-containing dinuclear and polymeric compounds with 9-arylcarbazole moiety and each of them exhibits interesting electronic and phosphorescence properties. Optical spectroscopy suggests that while the carbazolyl group is weak in electronic conjugation, the resulting organometallic materials show strong triplet emission with negligible fluorescence intensity at low temperatures. The reduced conjugation in the presence of carbazolyl unit shifts the absorption and the phosphorescence bands to the blue compared to the related systems with more conjugated aromatic and heteroaromatic spacers. These new polymer systems enable the study of the relationship between chemical structure and triplet energy levels in conjugated polymers and materials and such an investigation is desirable for optoelectronic applications that harvest the spin-forbidden phosphorescent state for more efficient light emission.

4. Experimental

4.1. General procedures

All the reactions were performed under an atmosphere of nitrogen using standard Schlenk techniques, but no special precautions were taken to exclude oxygen during workup. Analytical grade solvents were purified by distillation over appropriate drying agent prior to use. All reagents and chemicals, unless otherwise stated, were purchased from commercial sources and used as received. The compounds *trans*-[PtPh(Cl)(PEt_3)$_2$] [30], *trans*-[$PtCl_2$-(PBu_3)$_2$] [31], 9-arylcarbazole [32] and 3,6-dibromo-9-(*p*-methoxyphenyl)carbazole [32] were prepared according to literature methods. *Caution!* Organomercurials are extremely toxic, and all experimentation involving these

Table 6
Experimental values of various transition energies among the S_0, S_1 and T_1 levels and intersystem crossing efficiencies of platinum(II), gold(I) and mercury(II) di-ynes and poly-ynes in the solid state at 11 K

Compound	$S_1 \rightarrow S_0$	$S_0 \rightarrow S_1$	$T_1 \rightarrow S_0$	$T_1 \rightarrow S_0$[a]	$\Delta E(S_1 \rightarrow S_0, T_1 \rightarrow S_0)$[b]
1a	3.06	3.49	2.68	2.73	310
1b	3.07	3.50	2.68	2.74	183
2a	3.10	3.71	2.72	2.80	108
2b	3.09	3.71	2.73	2.81	95
3a	3.17	3.64	2.72	2.86	61
3b	3.18	3.65	2.72	2.85	85
4a	3.23	3.75	2.76	2.90	19[c]
4b	3.25	3.76	2.75	2.92	9[c]

All energy units are in eV.
[a] The data were estimated from the PL spectra in CH_2Cl_2 glass at 77 K.
[b] Ratio of the intensities of triplet emission to singlet emission at 11 K.
[c] The presence of broad aggregate emission band will probably lead to some uncertainties and underestimation of the data.

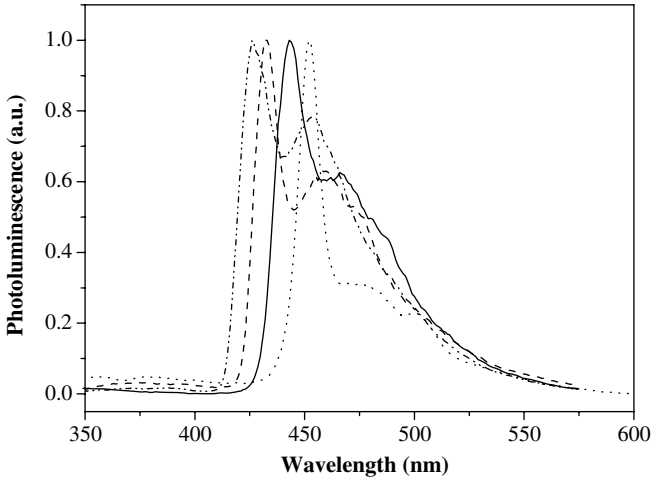

Fig. 10. Phosphorescence spectra of **1a** (···), **2a** (- - -), **3a** (—) and **4a** (-·-·-) at 77 K.

reagents should be performed in a well-vented hood. Glasswares were oven-dried at about 120 °C. Separation or purification of products were achieved by preparative thin-layer chromatography (TLC) on glass plates (20 cm × 20 cm) coated with Merck Kieselgel $60GF_{254}$ prepared in our laboratory (0.7 mm) or column chromatography on silica.

Infrared spectra were recorded in dichloromethane on a Perkin Elmer FTIR 550 spectrometer, using CaF_2 cells with a 0.5 cm path length. The ^1H, ^{13}C and ^{31}P NMR spectra were recorded on a JEOL JNM-EX270 FT NMR system or a VARIAN 400 MHz NMR spectrometer, using deuterated solvents as the lock and reference. Chemical shifts were reported in ppm relative to $SiMe_4$ for ^1H and ^{13}C nuclei and 85% H_3PO_4 for ^{31}P nucleus. The positive-ion fast atom bombardment (FAB) mass spectra were obtained using Finnigan-MAT SSQ710 mass spectrometer. Electronic absorption spectra were obtained with a Hewlett Packard 8453 UV–Vis spectrometer. The solution emission spectra were measured on a PTI Fluorescence Master Series QM1 spectrophotometer. For solid state emission spectral measurement, the 325 nm line of a He–Cd laser was used as an excitation source. The photoluminescence spectra were analyzed by a 0.25 m focal length double monochromator with a Peltier cooled photomultiplier tube and processed with a lock-in amplifier. For the low temperature measurements, samples were mounted in a closed-cycle cryostat (Oxford CC1104) in which the temperature can be adjusted from 10 to 330 K. The fluorescence quantum yields (Φ_F) were determined in dichloromethane solutions at 290 K against the anthracene standard ($\Phi_F = 0.27$) [33]. The molecular weights of the polymers were determined by GPC (HP 1050 series HPLC with visible wavelength and fluorescent detectors) in THF using polystyrene standards and thermal analyses were performed with the Perkin–Elmer Pyris Diamond DSC-50 and Perkin TGA6 thermal analyzers at a heating rate of 20 °C/min.

4.2. Preparations of ligands

4.2.1. Synthesis of 3,6-bis(trimethylsilylethynyl)-9-(p-methoxyphenyl)carbazole

To an ice-cooled mixture of 3,6-dibromo-9-(*p*-methoxyphenyl)carbazole (750.0 mg, 1.74 mmol) in freshly distilled $^iPr_2NH$ (50 cm^3) under nitrogen, CuI (4.4 mg, 0.02 mmol), $Pd(OAc)_2$ (4.2 mg, 0.02 mmol) and PPh_3 (12.9 mg, 0.05 mmol) were added. The solution was stirred for 20 min and $Me_3SiC{\equiv}CH$ (427.2 mg, 4.35 mmol) was then added. The reaction mixture was stirred for 30 min in an ice bath before being warmed to room temperature. After reacting for 30 min at room temperature, the mixture was heated to 85 °C for 20 h. The completion of the reaction was verified by IR spectroscopy and spot TLC. The solvent was evaporated to dryness, the residue redissolved in Et_2O (100 cm^3) and the solution washed with dilute HCl (2×100 cm^3) followed by water (2×100 cm^3). Upon filtration through a short pad of celite, the filtrate was washed with saturated $NaHCO_3$ (2×100 cm^3) and water (2×100 cm^3) and the resulting organic solution was dried over anhydrous $MgSO_4$. The brown–yellow residue was chromatographed over a silica gel column using hexane as the eluent. The crude product was eluted as a light yellow band and the pure fraction was evaporated to dryness and recrystallized from a solvent mixture of hexane and CH_2Cl_2 to give 3,6-bis(trimethylsilylethynyl)-9-(*p*-methoxyphenyl)carbazole as a yellow solid in 90% yield (730.0 mg). IR (CH_2Cl_2): ν(C≡C) 2152 cm^{-1}. ^1H NMR ($CDCl_3$): δ 8.18 (s, br, 2H, Ar), 7.40 (d, $J = 8.1$ Hz, 2H, Ar), 7.09–7.00 (m, 4H, Ar), 6.87 (d, $J = 8.1$ Hz, 2H, Ar), 3.73 (s, 3H, OMe), 0.30 (s, 18H, $SiMe_3$) ppm. ^{13}C NMR ($CDCl_3$): δ 158.52, 140.68, 129.68, 128.53, 127.59, 123.99, 121.94, 114.59, 114.22, 109.27 (Ar), 105.96, 91.81 (C≡C), 55.06 (OMe) ppm. FAB-MS: *m/z* 466 [M^+]. Anal. Calc. for $C_{29}H_{31}NOSi_2$: C, 74.79; H, 6.71; N, 3.01. Found: C, 74.62; H, 6.50; N, 2.93%.

4.2.2. Synthesis of **Ia**

3,6-Bis(trimethylsilylethynyl)-9-(*p*-methoxyphenyl)carbazole (782.5 mg, 1.68 mmol) was dissolved in Et_2O (10 cm^3) to give a colorless solution and a catalytic amount of K_2CO_3 (232.2 mg, 1.68 mmol) in MeOH (10 cm^3) was added. A milky solution was obtained after 24 h at room temperature. The solvent was removed and the crude product was purified by silica column chromatography eluting with CH_2Cl_2 to afford a light yellow solid of 3,6-diethynyl-9-(*p*-methoxyphenyl)carbazole in 88% yield (480.0 mg). IR (CH_2Cl_2): ν(C≡C) 2107, ν(C≡CH) 3301 cm^{-1}. ^1H NMR ($CDCl_3$): δ 8.22 (s, br, 2H, Ar), 7.50 (d, $J = 8.1$ Hz, 2H, Ar), 7.32–7.30 (m, 2H, Ar), 7.18 (d, $J = 8.1$ Hz, 2H, Ar), 7.05 (d, $J = 8.1$ Hz, 2H, Ar), 3.86 (s, 3H, OMe), 3.07 (s, 2H, C≡CH) ppm. ^{13}C NMR ($CDCl_3$): δ 159.00, 141.33, 130.18, 128.95, 128.17, 124.47, 122.27, 115.04, 113.41, 109.82 (Ar), 84.54, 75.72 (C≡C), 55.55 (OMe) ppm. FAB-MS: *m*/*z* 321 [M^+]. Anal. Calc. for $C_{23}H_{15}NO$: C, 85.96; H, 4.70; N, 4.36. Found: C, 85.74; H, 4.60; N, 4.25%.

4.2.3. Synthesis of 3,6-dibromo-9-(p-chlorophenyl)carbazole

In the absence of light, a solution of NBS (1.05 g, 5.90 mmol) in DMF (30 cm^3) was slowly added dropwise to an ice-cooled solution of 9-(*p*-chlorophenyl)carbazole (0.71 g, 2.57 mmol) in DMF (30 cm^3), and the mixture was stirred for 4 h at room temperature. Ice was added to the mixture and a white solid was precipitated. The crude product was washed with water (3×15 cm^3) and recrystallized from toluene/hexane to afford 3,6-dibromo-9-(*p*-chlorophenyl)carbazole (0.97 g, 87%). ^1H NMR ($CDCl_3$): δ 8.17 (s, br, 2H, Ar), 7.50 (d, $J = 8.0$ Hz, 2H, Ar), 7.51–7.48 (m, 2H, Ar), 7.43 (d, $J = 8.0$ Hz, 2H, Ar), 7.20 (d, $J = 8.0$ Hz, 2H, Ar) ppm. ^{13}C NMR ($CDCl_3$): δ 139.68, 135.30, 133.82, 130.38, 129.52, 128.23, 124.00, 123.29, 113.32, 111.26 (Ar) ppm. FAB-MS: *m*/*z* 436 [M^+]. Anal. Calc. for $C_{18}H_{10}NBr_2Cl$: C, 49.64; H, 2.31; N, 3.22. Found: C, 49.45; H, 2.10; N, 3.03%.

4.2.4. Synthesis of 3,6-bis(trimethylsilylethynyl)-9-(p-chlorophenyl)carbazole

CuI (4.6 mg, 0.02 mmol), $Pd(OAc)_2$ (4.4 mg, 0.02 mmol) and PPh_3 (13.4 mg, 0.05 mmol) were introduced to an ice-cooled mixture of 3,6-dibromo-9-(*p*-chlorophenyl)carbazole (953.1 mg, 2.19 mmol) in freshly distilled $^iPr_2NH$ (50 cm^3) under nitrogen.. The solution was stirred for 20 min. $Me_3SiC{\equiv}CH$ (537.3 mg, 5.47 mmol) was then added and the reaction mixture was stirred for 30 min in an ice bath before being warmed to room temperature. After reacting for 30 min at room temperature, the mixture was heated to 85 °C for 20 h. The solvent was evaporated to dryness, the residue redissolved in Et_2O (100 cm^3) and the solution washed with dilute HCl (2×100 cm^3) followed by water (2×100 cm^3). Upon filtration through a pad of celite, the filtrate was treated with saturated $NaHCO_3$ (2×100 cm^3) and water (2×100 cm^3) and the resulting organic solution was dried over $MgSO_4$. The brown–yellow residue following evaporation was chromatographed over a silica gel column by elution with hexane. The desired product was isolated as a yellow solid in 77% yield (0.79 g) after recrystallization from hexane/CH_2Cl_2. IR (CH_2Cl_2): ν(C≡C) 2151 cm^{-1}. ^1H NMR ($CDCl_3$): δ 8.18 (s, br, 2H, Ar), 7.49 (d, $J = 8.9$ Hz, 2H, Ar), 7.45–7.42 (m, 2H, Ar), 7.24 (d, $J = 8.9$ Hz, 2H, Ar), 7.10 (d, $J = 8.6$ Hz, 2H, Ar), 0.35 (s, 18H, $SiMe_3$) ppm. ^{13}C NMR ($CDCl_3$): δ 140.02, 134.71, 133.36, 133.07, 129.84, 129.73, 127.59, 124.09, 122.30, 114.82 (Ar), 109.10, 105.63 (C≡C), 0.00 ($SiMe_3$) ppm. FAB-MS: *m*/*z* 470 [M^+]. Anal. Calc. for $C_{28}H_{28}NClSi_2$: C, 71.53; H, 6.00; N, 2.98. Found: C, 71.35; H, 5.84; N, 3.00%.

4.2.5. Synthesis of **Ib**

3,6-Bis(trimethylsilylethynyl)-9-(*p*-chlorophenyl)carbazole (789.1 mg, 1.68 mmol) was dissolved in Et_2O (10 cm^3) to give a colorless solution and a catalytic amount of K_2CO_3 (232.0 mg, 1.68 mmol) in MeOH (10 cm^3) was added. A milky solution was obtained after 24 h at room temperature. The solvent was removed and the crude product was purified by silica column chromatography eluting with CH_2Cl_2 to afford a light yellow solid of 9-(*p*-chlorophenyl)-3,6-diethynylcarbazole in 94% yield (520.0 mg). IR (CH_2Cl_2): ν(C≡C) 2107, ν(C≡CH) 3301 cm^{-1}. ^1H NMR ($CDCl_3$): δ 8.19 (s, br, 2H, Ar), 7.55–7.47 (m, 4H, Ar), 7.39–7.36 (d, $J = 8.6$ Hz, 2H, Ar), 7.22–7.18 (d, $J = 8.6$ Hz, 2H, Ar), 3.09 (s, 2H, C≡CH) ppm. ^{13}C NMR ($CDCl_3$): δ 140.62, 135.01, 133.56, 130.34, 130.13, 128.05, 124.56, 122.60, 114.01, 109.62 (Ar), 84.29, 75.99 (C≡C) ppm. FAB-MS: *m*/*z* 326 [M^+]. Anal. Calc. for $C_{22}H_{12}NCl$: C, 81.11; H, 3.71; N, 4.30. Found: C, 80.98; H, 3.55; N, 4.10%.

4.3. Preparations of polymers and complexes

4.3.1. Synthesis of **1a**

A mixture of *trans*-[$PtCl_2(PBu_3)_2$] (100.9 mg, 0.15 mmol) and 1 equivalent of **Ia** (48.4 mg, 0.15 mmol) was dissolved in $^iPr_2NH/CH_2Cl_2$ (50 cm^3, 1:1, v/v) and CuI (3.0 mg) was subsequently added. After stirring at room temperature for 15 h, all the volatile compounds were removed under reduced pressure. The residue was redissolved in CH_2Cl_2 and filtered through a short silica column using CH_2Cl_2 as eluent to give a yellow solution. After the removal of solvent by a rotary evaporator, a yellow powder of the title polymer was obtained in 65% yield (89.9 mg) after reprecipitation from a CH_2Cl_2/MeOH mixture. IR (CH_2Cl_2): ν(C≡C) 2098 cm^{-1}. ^1H NMR ($CDCl_3$): δ 8.00 (m, 2H, Ar), 7.45–7.43 (m, 2H, Ar), 7.34–7.32 (m, 2H, Ar), 7.17–7.14 (m, 2H, Ar), 7.10–7.08 (m, 2H, Ar), 3.91 (s, 3H, OMe), 2.23 (m, 12H, PCH_2), 1.68 (m, 12H, PCH_2CH_2), 1.54–1.48 (m, 12H, CH_2CH_3), 0.99–0.94 (m, 18H, CH_2CH_3) ppm. ^{13}C NMR ($CDCl_3$): δ 158.54, 139.33, 130.50, 129.14, 128.31, 122.88, 122.10, 120.58, 114.89, 109.06 (Ar) 109.33, 104.74 (C≡C), 55.58 (OMe), 26.42, 24.48, 23.98, 13.91 (Bu) ppm. ^{31}P NMR ($CDCl_3$): δ 4.10

($J_{Pt-P} = 2375$ Hz) ppm. Anal. Calc. for $(C_{47}H_{67}NOP_2Pt)_n$: C, 61.42; H, 7.35; N, 1.52. Found: C, 61.20; H, 7.03; N, 1.35%.

4.3.2. Synthesis of **1b**

A mixture of *trans*-$[PtCl_2(PBu_3)_2]$ (81.3 mg, 0.12 mmol) and 1 equivalent of **Ib** (39.5 mg, 0.12 mmol) was dissolved in $^iPr_2NH/CH_2Cl_2$ (50 cm^3, 1:1, v/v) and CuI (3.0 mg) was subsequently added. After stirring at room temperature for 15 h, a brown–yellow powder was obtained in 78% (87.8 mg) after the same workup procedures as described above for **1a**. IR (CH_2Cl_2): ν(C≡C) 2101 cm^{-1}. ^1H NMR ($CDCl_3$): δ 7.98 (m, 2H, Ar), 7.57–7.47 (m, 4H, Ar), 7.34 (m, 2H, Ar), 7.22–7.19 (m, 2H, Ar), 2.24 (m, 12H, PCH_2), 1.71 (m, 12H, PCH_2CH_2), 1.60–1.40 (m, 12H, CH_2CH_3), 1.01–0.92 (m, 18H, CH_2CH_3) ppm. ^{13}C NMR ($CDCl_3$): δ 138.58, 136.39, 132.48, 129.93, 129.28, 128.04, 123.25, 122.09, 121.14, 108.95 (Ar), 109.14, 105.25 (C≡C), 26.54, 24.66, 24.19, 13.95 (Bu) ppm. ^{31}P NMR ($CDCl_3$): δ 4.20 ($J_{Pt-P} = 2368$ Hz) ppm. Anal. Calc. for $(C_{46}H_{64}NClP_2Pt)_n$: C, 59.83; H, 6.99; N, 1.52. Found: C, 59.55; H, 6.78; N, 1.34%.

4.3.3. Synthesis of **2a**

Treatment of **Ia** (34.0 mg, 0.11 mmol) with two equivalents of *trans*-$[PtPh(Cl)(PEt_3)_2]$ (115.0 mg, 0.22 mmol) at room temperature for 15 h, in the presence of CuI (3.0 mg), in $^iPr_2NH/CH_2Cl_2$ (30 cm^3, 1:1, v/v) gave the title complex as a yellow solid in 63% yield (89.0 mg) after purification on silica TLC plates using hexane/CH_2Cl_2 (40:60, v/v) as eluent. IR (CH_2Cl_2): ν(C≡C) 2095 cm^{-1}. ^1H NMR ($CDCl_3$): δ 8.03 (s, 2H, Ar), 7.44–7.40 (m, 3H, Ar), 7.38–7.34 (m, 5H, Ar), 7.16–7.14 (m, 2H, Ar), 7.09–7.07 (m, 2H, Ar), 6.97 (t, $J = 7.4$ Hz, 4H, Ar), 6.82 (t, $J = 7.2$ Hz, 2H, Ar), 3.90 (s, 3H, OMe), 1.85–1.77 (m, 24H, PCH_2CH_3), 1.17–1.06 (m, 36H, PCH_2CH_3) ppm. ^{13}C NMR ($CDCl_3$): δ 158.47, 156.78, 139.26, 130.57, 129.09, 128.22, 127.20, 122.93, 122.21, 121.07, 120.76, 115.02, 114.85, 109.02 (Ar) 110.75, 109.23 (C≡C), 55.55 (OMe), 15.09, 8.05 (Et) ppm. ^{31}P NMR ($CDCl_3$): δ 10.87 ($J_{Pt-P} = 2643$ Hz) ppm. FAB-MS: m/z 1336 [M^+]. Anal. Calc. for $C_{59}H_{83}NOP_4Pt_2$: C, 53.03; H, 6.26; N, 1.05. Found: C, 52.88; H, 6.03; N, 0.96%.

4.3.4. Synthesis of **2b**

Treatment of **Ib** (37.0 mg, 0.11 mmol) with two equivalents of *trans*-$[PtPh(Cl)(PEt_3)_2]$ (123.6 mg, 0.22 mmol) at room temperature for 15 h, in the presence of CuI (3 mg), in $^iPr_2NH/CH_2Cl_2$ (30 mL, 1:1, v/v) gave the title complex as a yellow solid in 55% yield (79.2 mg) after purification on silica TLC plates using hexane/CH_2Cl_2 (40:60, v/v) as eluent. IR (CH_2Cl_2): ν(C≡C) 2092 cm^{-1}. ^1H NMR ($CDCl_3$): δ 8.01 (s, 2H, Ar), 7.55–7.45 (m, 6H, Ar), 7.38–7.34 (m, 4H, Ar), 7.19 (d, $J = 8.4$ Hz, 2H, Ar), 6.97 (t, $J = 7.3$ Hz, 4H, Ar), 6.81 (t, $J = 7.0$ Hz, 2H, Ar) 1.84–1.77 (m, 24H, PCH_2CH_3), 1.19–1.04 (m, 36H, PCH_2CH_3) ppm. ^{13}C NMR ($CDCl_3$): δ 156.42, 139.14, 138.41, 136.47, 132.34, 129.83, 129.20, 127.92, 127.15, 123.29, 122.19, 121.36, 121.07, 108.87 (Ar), 110.51, 109.85 (C≡C), 15.28, 8.36 (Et) ppm. ^{31}P NMR ($CDCl_3$): δ 11.35 ($J_{Pt-P} = 2602$ Hz) ppm. FAB-MS: m/z 1340 [M^+]. Anal. Calc. for $C_{58}H_{80}NClP_4Pt_2$: C, 51.96; H, 6.01; N, 1.04. Found: C, 51.77; H, 5.80; N, 0.93%.

4.3.5. Synthesis of **3a**

$Au(PPh_3)Cl$ (103.8 mg, 0.21 mmol) was dissolved in MeOH (15 cm^3), and **Ia** (28.1 mg, 0.09 mmol) in CH_2Cl_2 (5 cm^3) was added. Then, 0.25 M NaOMe (1.4 cm^3, 0.36 mmol) was added into the mixture, and the mixture was allowed to stir at room temperature under nitrogen for 2 h. The product was precipitated out and centrifuged. The solvent was removed and the product was air-dried to obtain the title product as a yellow solid (95.5 mg, 88%). IR (CH_2Cl_2): ν(C≡C) 2113 cm^{-1}. ^1H NMR ($CDCl_3$): δ 8.28 (s, 2H, Ar), 7.61–7.39 (m, 36H, Ar), 7.18 (d, $J = 8.4$ Hz, 2H, Ar), 3.89 (s, 3H, OMe) ppm. ^{13}C NMR ($CDCl_3$): δ 158.68, 140.38, 134.29, 134.08, 131.38, 130.50, 130.14, 129.80, 129.33, 128.88, 128.27, 124.38, 122.62, 114.91 (Ar), 115.97, 109.28 (C≡C) 55.60 (OMe) ppm. ^{31}P NMR ($CDCl_3$): δ 43.91 ppm. FAB-MS: m/z 1238 [M^+]. Anal. Calc. for $C_{59}H_{43}NOP_2Au_2$: C, 57.25; H, 3.50; N, 1.13. Found: C, 57.01; H, 3.26; N, 0.99%.

4.3.6. Synthesis of **3b**

$Au(PPh_3)Cl$ (105.3 mg, 0.21 mmol) was dissolved in MeOH (15 cm^3), and **Ib** (32.5 mg, 0.09 mmol) in CH_2Cl_2 (5 cm^3) was added. Subsequently, 0.25 M NaOMe (1.4 cm^3, 0.36 mmol) was added into the mixture, and the mixture was allowed to stir at room temperature under nitrogen for 2 h. The product was precipitated out and centrifuged. The solvent was removed and the product was air-dried to obtain a yellow solid (108.1 mg, 95%). IR (CH_2Cl_2): ν(C≡C) 2113 cm^{-1}. ^1H NMR ($CDCl_3$): δ 8.25 (s, 2H, Ar), 8.25–7.40 (m, 36H, Ar), 7.21 (d, $J = 8.1$ Hz, 2H, Ar) ppm. ^{13}C NMR ($CDCl_3$): δ 139.71, 135.83, 134.33, 134.12, 132.93, 131.41, 130.73, 130.16, 129.94, 129.09, 128.92, 128.17, 124.50, 123.02 (Ar) 116.62, 109.16 (C≡C) ppm. ^{31}P NMR ($CDCl_3$): δ 43.86 ppm. FAB-MS: m/z 1242 [M^+]. Anal. Calc. for $C_{58}H_{40}ClNP_2Au_2$: C, 56.08; H, 3.25; N, 1.13. Found: C, 55.86; H, 3.01; N, 1.10%.

4.3.7. Synthesis of **4a**

The di-yne **Ia** (46.9 mg, 0.15 mmol) in MeOH (10 cm^3) was first combined with MeHgCl (88.5 mg, 0.35 mmol) in MeOH (10 cm^3) and 0.20 M basic MeOH (2.9 cm^3, 0.58 mmol) was subsequently added to give a pale-yellow suspension. The solvents were then decanted and a light-yellow solid of the title compound was washed with MeOH (2×20 cm^3) and air-dried (90.8 mg, 83%). IR (CH_2Cl_2): ν(C≡C) 2131 cm^{-1}. ^1H NMR ($CDCl_3$): δ 8.21 (s, 2H, Ar), 7.52 (m, 2H, Ar), 7.42 (d, $J = 8.9$ Hz, 2H, Ar), 7.22 (d, $J = 8.6$ Hz, 2H, Ar), 7.11 (d, $J = 8.9$ Hz, 2H, Ar), 3.91 (s, 3H, OMe), 0.70 (s, $J = 146.1$ Hz, 6H, MeHg) ppm. ^{13}C NMR ($CDCl_3$): δ 159.05, 141.09, 140.80,

Table 7
Summary of crystal structure data for **2a**, **3a** and **4b**

	2a	**3a**	**4b**
Empirical formula	$C_{59}H_{83}NOP_4Pt_2$	$C_{59}H_{43}NOP_2Au$	$C_{24}H_{16}NClHg_2$
Molecular weight	1336.32	1237.82	755.01
Crystal size (mm)	$0.30 \times 0.24 \times 0.10$	$0.28 \times 0.20 \times 0.18$	$0.25 \times 0.20 \times 0.10$
Crystal system	Triclinic	Monoclinic	Monoclinic
Space group	$P\bar{1}$	$P2_1/c$	$P2/c$
a (Å)	18.0068(11)	20.334(10)	16.3623(12)
b (Å)	18.2384(10)	16.745(8)	16.7364(12)
c (Å)	19.6550(12)	14.982(7)	7.5600(6)
α (°)	99.5020(10)	90	90
β (°)	90.8620(10)	111.041(9)	97.871(2)
γ (°)	103.3270(10)	90	90
U (Å^3)	6185.5(6)	4761(4)	2050.8(3)
μ (Mo Kα) (mm^{-1})	4.657	6.266	15.094
D_{calc} (g cm^{-3})	1.435	1.727	2.445
Z	4	4	4
$F(000)$	2672	2400	1376
θ Range (°)	1.70–25.00	1.90–25.00	1.75–25.00
Reflections collected	31,212	23,286	10,104
Unique reflections	21,427	8366	3607
R_{int}	0.0501	0.0355	0.0883
Observed reflections [$I > 2\sigma(I)$]	9961	6752	2056
Number of parameters	1207	586	259
R_1, $wR_2[I > 2\sigma(I)]$	0.0630, 0.1314	0.0341, 0.0892	0.0546, 0.1174
R_1, wR_2 (all data)	0.1547, 0.1718	0.0481, 0.0982	0.1189, 0.1435
Goodness-of-fit on F^2	0.975	1.024	0.999
Residual extrema in final difference map (e Å^{-3})	1.822 to −2.317 (close to Pt)	2.204 to −1.154 (close to Au)	0.872 to −0.878

130.32, 129.32, 128.33, 124.37, 122.55, 115.11, 114.47 (Ar), 109.84, 106.36 (C≡C), 55.65 (OMe), 7.29 (MeHg) ppm. FAB-MS: m/z 751 [M$^+$]. Anal. Calc. for $C_{25}H_{19}NOHg_2$: C, 40.00; H, 2.55; N, 1.87. Found: C, 39.88; H, 2.30; N, 1.58%.

4.3.8. Synthesis of *4b*

The ligand **Ib** (44.8 mg, 0.14 mmol) in MeOH (10 cm^3) was first combined with MeHgCl (82.9 mg, 0.33 mmol) in MeOH (10 cm^3) and 0.20 M basic MeOH (2.8 cm^3, 0.56 mmol) was subsequently added to give a pale-yellow suspension. The solvents were then decanted and a pale yellow solid of the title compound was washed with MeOH (2×20 cm^3) and air-dried (92.1 mg, 89%). IR (CH_2Cl_2): ν(C≡C) 2134 cm^{-1}. ^{1}H NMR ($CDCl_3$): δ 8.22 (s, 2H, Ar), 7.61 (m, 2H, Ar), 7.57 (m, 2H, Ar), 7.49 (d, $J = 8.6$ Hz, 2H, Ar), 7.24 (d, $J = 8.9$ Hz, 2H, Ar), 0.72 (s, $J = 145.3$ Hz, 6H, MeHg) ppm. ^{13}C NMR ($CDCl_3$): δ 141.06, 140.29, 135.21, 133.44, 130.39, 130.10, 128.12, 124.34, 122.77, 114.96 (Ar), 109.57, 105.91 (C≡C), 7.17 (MeHg) ppm. FAB-MS: m/z 755 [M$^+$]. Anal. Calc. for $C_{24}H_{16}NClHg_2$: C, 38.18; H, 2.14; N, 1.86. Found: C, 37.96; H, 2.02; N, 1.55%.

5. Crystallography

Single crystals of **2a**, **3a** and **4b** suitable for X-ray diffraction work were obtained by slow evaporation of their respective solutions in CH_2Cl_2/hexane at room temperature. Crystal data, data collection parameters and results of the analyses are listed in Table 7. Geometric and intensity data were collected at room temperature on a Bruker Axs Smart 1000 CCD area detector using graphite-monochromated Mo Kα radiation ($\lambda = 0.71073$ Å). The collected frames were processed with the software SAINT [34], and an absorption correction was applied (SADABS) [35] to the collected reflections. The structure was solved by the Patterson or direct methods (SHELXTL) [36] in conjunction with standard difference Fourier techniques and subsequently refined by full-matrix least-squares analyses on F^2. All non-hydrogen atoms were assigned with anisotropic displacement parameters.

Acknowledgements

Financial support from a CERG Grant from the Hong Kong Research Grants Council of the Hong Kong SAR, P.R. China (Project No. HKBU2022/03P) and Hong Kong Baptist University is gratefully acknowledged.

Appendix A. Supplementary material

Crystallographic data (comprising hydrogen atom coordinates, thermal parameters and full tables of bond lengths and angles) for the structural analysis has been deposited with the Cambridge Crystallographic Centre (Deposition Nos. 602241–602243). Copies of this information may be obtained free of charge from The Director, CCDC, 12 Union Road, Cambridge CB2 1EZ, UK (Fax: + 44 1223 336 033; e-mail: deposit@ccdc.cam.ac.uk or

www: http://www.ccdc.cam.ac.uk). Supplementary data associated with this article can be found, in the online version, at doi:10.1016/j.jorganchem.2006.06.006.

References

[1] (a) P. Strohriegl, J.V. Grazulevicius, Adv. Mater. 14 (2002) 1439;
(b) P. Kunda, K.R. Justin Thomas, J.T. Lin, Y.-T. Tao, C.-H. Chien, Adv. Funct. Mater. 13 (2003) 445;
(c) K.R. Justin Thomas, J.-T. Lin, Y.-T. Tao, C.-W. Ko, Adv. Mater. 12 (2000) 1949;
(d) K.R. Justin Thomas, J.-T. Lin, Y.-T. Tao, C.-W. Ko, J. Am. Chem. Soc. 123 (2001) 9404;
(e) F. Sanda, T. Nakai, N. Kobayashi, T. Masuda, Macromolecules 37 (2004) 2703;
(f) S. Maruyama, X.-T. Tao, H. Hokari, T. Noh, Y. Zhang, T. Wada, H. Sasabe, H. Suzuki, T. Watanabe, S. Miyata, J. Mater. Chem. 9 (1999) 893;
(g) J. Chung, B. Choi, H.H. Lee, Appl. Phys. Lett. 74 (1999) 3645;
(h) X.-T. Tao, H. Suzuki, T. Wada, H. Saade, S. Miyata, Appl. Phys. Lett. 75 (1999) 1655.

[2] T. Tsutsui, M.J. Yang, M. Yahiro, K. Nakamura, T. Watanabe, T. Tsuji, M. Fukuda, T. Wakimoto, S. Miyaguchi, Jpn. J. Appl. Phys. 38 (1999) L1502.

[3] S. Lamanskey, P. Djurovich, D. Murphy, F. Abdel-Razzaq, H.E. Lee, C. Adachi, P.E. Burrows, S.R. Forrest, M.E. Thompson, J. Am. Chem. Soc. 123 (2001) 4304.

[4] D.F. O' Brien, M.A. Baldo, M.E. Thompson, S.R. Forrest, Appl. Phys. Lett. 74 (1999) 442.

[5] C. Adachi, M.A. Baldo, S.R. Forrest, S. Lamansky, M.E. Thompson, R.C. Kwong, Appl. Phys. Lett. 78 (2001) 1622.

[6] M.A. Baldo, S. Lamansky, P.E. Burrows, M.E. Thompson, S.R. Forrest, Appl. Phys. Lett. 75 (1999) 4.

[7] C. Adachi, R.C. Kwong, S.R. Forrest, Org. Electron. 2 (2001) 37.

[8] C. Adachi, R.C. Kwong, P. Djurovich, V. Adamovich, M.A. Baldo, M.E. Thompson, S.R. Forrest, Appl. Phys. Lett. 79 (2001) 2082.

[9] R.J. Holmes, S.R. Forrest, Y.J. Tung, R.C. Kwong, J.J. Brown, S. Garon, M.E. Thompson, Appl. Phys. Lett. 82 (2003) 2422.

[10] (a) A. Kimoto, J.-S. Cho, M. Higuchi, K. Yamamoto, Macromolecules 37 (2004) 5531;
(b) Z. Zhu, J.S. Moore, J. Org. Chem. 65 (2000) 116;
(c) F. Sanda, T. Kawaguchi, T. Masuda, Macromolecules 36 (2003) 2224;
(d) C. Xia, R.C. Advincula, Macromolecules 34 (2001) 5854;
(e) S. Maruyama, H. Hokari, T. Wada, H. Sasabe, Synthesis (2001) 1794;
(f) B.Z. Tang, H.Z. Chen, R.S. Xu, J.W.Y. Lam, K.K.L. Cheuk, H.N.C. Wong, M. Wang, Chem. Mater. 12 (2000) 213;
(g) Z.L. Xie, J.W.Y. Lam, C.F. Qiu, M. Wong, H.S. Kwok, B.Z. Tang, Polym. Mater. Sci. Eng. 89 (2003) 416;
(h) K. Brunner, A. van Dijken, H. Börner, J.J.A.M. Bastiaansen, N.M.M. Kiggen, B.M.W. Langeveld, J. Am. Chem. Soc. 126 (2004) 6035.

[11] (a) W.-Y. Wong, Coord. Chem. Rev. 249 (2005) 971, and references therein;
(b) N.D. McClenaghan, R. Passalacqua, F. Loiseau, S. Campagna, B. Verheyde, A. Hameurlaine, W. Dehaen, J. Am. Chem. Soc. 125 (2003) 5356;
(c) A.-C. Ribou, T. Wada, H. Saabe, Inorg. Chim. Acta 288 (1999) 134;
(d) C.-L. Ho, W.-Y. Wong, J. Organomet. Chem. 691 (2006) 395.

[12] (a) C.-H. Tao, K.M.-C. Wong, N. Zhu, V.W.-W. Yam, New J. Chem. 27 (2003) 150;
(b) W.-Y. Wong, G.-L. Lu, K.-H. Choi, J.-X. Shi, Macromolecules 35 (2002) 3506.

[13] (a) W.-Y. Wong, C.-K. Wong, G.-L. Lu, A.W.-M. Lee, K.-W. Cheah, J.-X. Shi, Macromolecules 36 (2003) 983;
(b) W.-Y. Wong, L. Liu, S.-Y. Poon, A.W.-M. Lee, K.-W. Cheah, J.-X. Shi, Macromolecules 37 (2004) 4496.

[14] (a) J. Hassan, M. Sévignon, C. Gozzi, E. Schulz, M. Lemaire, Chem. Rev. 102 (2002) 1359, and references cited therein;
(b) M. Martínez-Palau, E. Perea, F. López-Calahorra, D. Velasco, Lett. Org. Chem. 1 (2004) 231.

[15] (a) K. Sonogashira, Y. Tohda, N. Hagihara, Tetrahedron Lett. (1975) 4476;
(b) S. Takahashi, Y. Kuroyama, K. Sonogashira, N. Hagihara, Synthesis (1980) 627.

[16] (a) W.-Y. Wong, J. Inorg. Organomet. Polym. Mater. 15 (2005) 197, and references cited therein;
(b) W.-Y. Wong, K.-H. Choi, G.-H. Lu, Macromol. Rapid Commun. 22 (2001) 461;
(c) N. Chawdhury, A. Köhler, R.H. Friend, W.-Y. Wong, J. Lewis, M. Younus, P.R. Raithby, T.C. Corcoran, M.R.A. Al-Mandhary, M.S. Khan, J. Chem. Phys. 110 (1999) 4963;
(d) H.F. Wittmann, R.H. Friend, M.S. Khan, J. Lewis, J. Chem. Phys. 101 (1994) 2693;
(e) B.F.G. Johnson, A.K. Kakkar, M.S. Khan, J. Lewis, A.E. Dray, R.H. Friend, F. Wittmann, J. Mater. Chem. 1 (1991) 485;
(f) A.K. Kakkar, M.S. Khan, N.J. Long, J. Lewis, P.R. Raithby, P. Nguyen, T.B. Marder, F. Wittmann, R.H. Friend, J. Mater. Chem. 4 (1994) 1227.

[17] (a) W.-Y. Wong, K.-H. Choi, G.-L. Lu, J.-X. Shi, P.-Y. Lai, S.-M. Chan, Z. Lin, Organometallics 20 (2001) 5446;
(b) B. Li, B. Ahrens, K.-H. Choi, M.S. Khan, P.R. Raithby, P.J. Wilson, W.-Y. Wong, CrystEngComm. 4 (2002) 405;
(c) R.J. Puddephatt, Coord. Chem. Rev. 216–217 (2001) 313;
(d) R.J. Puddephatt, Chem. Commun. (1998) 1055;
(e) H.-Y. Chao, W. Lu, Y. Li, M.C.W. Chan, C.-M. Che, K.-K. Cheung, N. Zhu, J. Am. Chem. Soc. 124 (2002) 14696.

[18] (a) F. Bolletta, D. Fabbri, M. Lombardo, L. Prodi, C. Trombini, N. Zaccheroni, Organometallics 15 (1996) 2415;
(b) W.-Y. Wong, G.-L. Lu, L. Li, J.-X. Shi, Z. Lin, Eur. J. Inorg. Chem. (2004) 2066.

[19] (a) W.-Y. Wong, S.-M. Chan, K.-H. Choi, K.-W. Cheah, W.-K. Chan, Macromol. Rapid Commun. 21 (2000) 453;
(b) W.-Y. Wong, K.-H. Choi, K.-W. Cheah, J. Chem. Soc., Dalton Trans. (2000) 113;
(c) C.-H. Tao, N. Zhu, V.W.-W. Yam, Chem. Eur. J. 11 (2005) 1647;
(d) S. Szafert, J.A. Gladysz, Chem. Rev. 103 (2003) 4175;
(e) N.J. Long, C.K. Williams, Angew. Chem. Int. Ed. 42 (2003) 2586, and references cited therein.

[20] (a) N.W. Alcock, P.A. Lampe, P. Moore, J. Chem. Soc., Dalton Trans. (1980) 1471;
(b) C.A. Ghilardi, S. Midollini, A. Orlandini, A. Vacca, J. Chem. Soc., Dalton Trans. (1993) 3117.

[21] (a) P. Pyykko, Chem. Rev. 97 (1997) 597, and references cited therein;
(b) K.R. Flower, V.J. Howard, S. Naguthney, R.G. Pritchard, J.E. Warren, A.T. McGown, Inorg. Chem. 41 (2002) 1907;
(c) S.S. Batsanov, J. Chem. Soc., Dalton Trans. (1998) 1541;
(d) A. Bondi, J. Phys. Chem. 68 (1964) 441.

[22] (a) S.J. Faville, W. Henderson, T.J. Mathieson, B.K. Nicholson, J. Organomet. Chem. 580 (1999) 363;
(b) D. Rais, D.M.P. Mingos, R. Vilar, A.J.P. White, D.J. Williams, Organometallics 19 (2000) 5209.

[23] (a) W.-Y. Wong, L. Liu, J.-X. Shi, Angew. Chem. Int. Ed. 42 (2003) 4064;
(b) W.-Y. Wong, K.-H. Choi, G.-L. Lu, Z. Lin, Organometallics 21 (2002) 4475.

[24] X. Wang, L. Andrews, Inorg. Chem. 43 (2004) 7146.

[25] W.-Y. Wong, G.-L. Lu, K.-H. Choi, J.-X. Shi, Macromolecules 35 (2002) 3506.

[26] L. Liu, S.-Y. Poon, W.-Y. Wong, J. Organomet. Chem. 690 (2005) 5036.

[27] (a) X. Zhao, T. Cardolaccia, R.T. Farley, K.A. Abboud, K.S. Schanze, Inorg. Chem. 44 (2005) 2619;
(b) U.H.F. Bunz, Chem. Rev. 100 (2000) 1605.
[28] (a) W.-Y. Wong, S.-Y. Poon, A.W.-M. Lee, J.-X. Shi, K.-W. Cheah, Chem. Commun. (2004) 2420;
(b) S.-Y. Poon, W.-Y. Wong, K.-W. Cheah, J.-X. Shi, Chem. Eur. J. 12 (2006) 2550.
[29] N. Chawdhury, A. Köhler, R.H. Friend, M. Younus, N.J. Long, P.R. Raithby, J. Lewis, Macromolecules 31 (1998) 722.
[30] J. Chatt, B.L. Shaw, J. Chem. Soc., (1960) 4020.
[31] J. Chatt, R.G. Hayter, J. Chem. Soc., Dalton Trans. (1961) 896.
[32] (a) W.-Y. Wong, L. Liu, D. Cui, L.M. Leung, C.-F. Kwong, T.-H. Lee, H.-F. Ng, Macromolecules 38 (2005) 4970;
(b) K. Brunner, A. van Dijken, H. Börner, J. Am. Chem. Soc. 126 (2004) 6035.
[33] W.R. Dawson, M.W. Windsor, J. Phys. Chem. 72 (1968) 3251.
[34] SAINT, Reference Manual; Siemens Energy and Automation, Madison, WI, 1994–1996.
[35] G.M. Sheldrick, SADABS, Empirical Absorption Correction Program, University of Göttingen, Germany, 1997.
[36] G.M. Sheldrick, SHELXTL, Reference Manual, ver. 5.1: Madison, WI, 1997.